

The Formation of Monodispersed Indium(III) Hydroxide Particles by Forced Hydrolysis at Elevated Temperature

Shuichi HAMADA,* Yoshiyuki KUDO, and Kazuhiro MINAGAWA

Department of Applied Chemistry, Faculty of Science, and Institute of Colloid and Interface Science, Science University of Tokyo, Kagurazaka, Shinjuku-ku, Tokyo 162

(Received July 20, 1989)

Rather poorly crystallized spherical particles of indium(III) hydroxide were produced by forced hydrolysis at 100 °C for 120 min under the conditions of 6.0×10^{-4} mol dm $^{-3}$ for indium(III) ions, 1.0×10^{-3} mol dm $^{-3}$ for nitric acid, and 1.25 for a concentration ratio, $[\text{SO}_4^{2-}]_t/[\text{In}^{3+}]_t$, respectively, having an average size of 0.48 μm with a relative standard deviation of 0.09. On the other hand, cubic particles of well-crystallized indium(III) hydroxide were yielded in a nitrate solution that was free from sulfate ions and at the same concentrations. The cubic particles grew through a polynuclear layers mechanism. Monomeric hydroxo complexes basically acted as precursors of the spherical particles, together partly with polymeric ones. The point of zero charge was estimated as being at the same pH (7.7) for both the hydroxide and oxide particles prepared from the nitrate system, in contrast to those of 7.0 and 5.4 for the respective particles obtained from the sulfate system.

Monodispersed particles of metal oxide and hydrous oxide have been prepared by several procedures. Particularly, the hydrolysis of metal ions at elevated temperatures has given well-defined corresponding oxide and hydrous oxide particles under suitable conditions.^{1–6} In this method, the morphology and composition of the particles depend on several parameters such as concentration, temperature, pH, and the kinds of anions present. It has been reported that sulfate ions are essential for producing monodispersed spherical particles of amorphous chromium(III),⁷ aluminium(III),⁸ and gallium(III)^{9,10} hydrous oxide by forced hydrolysis, whereas crystalline particles have been produced from the latter two metal nitrate and chloride solutions. The role of sulfate ions in the formation of such particles has been mentioned.^{7–12}

In the present work, the preparation of monodispersed indium(III) hydrous oxide particles was studied by an aging method, together with their formation process and surface properties.

Experimental

Materials. All of the reagents used in this work were of guaranteed grade and were employed without further purification. A stock solution of indium(III) was prepared by dissolving its nitrate salt in doubly distilled water with a known amount of nitric acid. The concentration of indium(III) was gravimetrically determined. The stock solution was kept in a cold place and did not show any visual change over three months. An aliquot of the stock solution was diluted at specified concentrations together with nitric acid. For a sulfate system, the concentration ratio of the total sulfate to the total indium(III), $[\text{SO}_4^{2-}]_t/[\text{In}^{3+}]_t$, was varied by up to 30 with potassium sulfate. The solution, thus prepared, was filtered through a membrane filter (0.2 μm in pore size) before aging.

Procedures. The freshly prepared solution (≈ 40 cm 3) was tightly sealed in a screw-capped Pyrex glass tube and then heated to 100 ± 0.5 °C at specified heating rates in an oil bath. The solution was rapidly quenched to room temperature after the desired period (from 30 to 220 min). Particles, thus

produced, were centrifuged at 1160 g and washed repeatedly with distilled water using ultrasonic equipment.

The morphology and size of the particles were observed with a scanning electron microscope (model ALPHA-10S). An X-ray powder diffractometer (Geigerflex model RAD III A) was used to identify the particles.

The concentration of indium(III) in a supernatant solution was followed at regular time intervals in order to study the reaction process after solids have been completely removed from the solution by centrifugation at 1160 g and filtration through a membrane filter (0.1 μm in pore size). The solution, thus obtained, did not show any Tyndall cone. The concentrations of monomeric and polymeric indium(III) species^{13–15} were determined spectrophotometrically using 8-quinolinol, as described in a previous paper.¹⁰

The point of zero charge of the particles was estimated by ordinary potentiometric titration. A sample (1.0 g) suspended in 50.0 cm 3 of a 4.00×10^{-3} mol dm $^{-3}$ sodium hydroxide solution was titrated very slowly with 1.00×10^{-1} mol dm $^{-3}$ nitric acid with vigorous stirring under a nitrogen atmosphere (flow rate of 100 cm 3 min $^{-1}$) at 25 ± 0.1 °C and an ionic strength of 0.10 mol dm $^{-3}$ (NaNO $_3$). The specific surface area was determined with a modified BET analyzer (model SA-1000). A surface analysis was carried out in order to identify species adsorbed on the surfaces of the particles using an X-ray photoelectron spectroscope (XPS), model ESCALAB Mk II.

Results

Particle Morphology Depending on Composition of Solution in Sulfate System. The effects of the total concentrations of indium(III) ions and nitric acid were examined on the formation of indium(III) hydrous oxide particles over the ranges from 2.0×10^{-4} to 8.0×10^{-3} mol dm $^{-3}$ and from 3.0×10^{-4} to 1.0×10^{-2} mol dm $^{-3}$, respectively, under a fixed concentration ratio, $[\text{SO}_4^{2-}]_t/[\text{In}^{3+}]_t$, of 1.25 at 100 ± 0.5 °C for 120 min. Initial pH values of these solutions ranged between 3.5 and 2.1 at room temperature.

Spherical particles of reasonably narrow size distribution were generated in fairly narrow concentration ranges, from 3.0×10^{-4} to 8.5×10^{-4} mol dm $^{-3}$ for $[\text{In}^{3+}]_t$

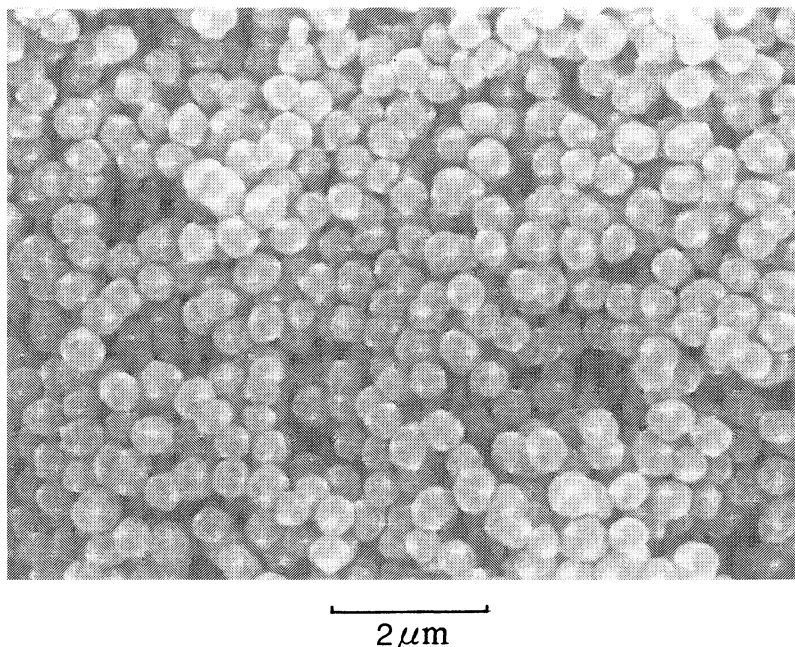


Fig. 1. Scanning electron micrograph of spherical indium(III) hydroxide particles obtained at 100°C for 120 min. Aging conditions: $[\text{In}^{3+}]_i = 6.0 \times 10^{-4} \text{ mol dm}^{-3}$, $[\text{HNO}_3] = 1.0 \times 10^{-3} \text{ mol dm}^{-3}$, and $[\text{SO}_4^{2-}]_i / [\text{In}^{3+}]_i = 1.25$.

and from 7.6×10^{-4} to $1.5 \times 10^{-3} \text{ mol dm}^{-3}$ for $[\text{HNO}_3]$, respectively, at an initial heating rate of $1^\circ \text{C min}^{-1}$. When the heating rate was faster than $1^\circ \text{C min}^{-1}$, the optimum conditions were limited to a very narrow composition range. On the other hand, only polydispersed particles appeared at a heating rate of $0.5^\circ \text{C min}^{-1}$. Thus, the specified heating rate of $1^\circ \text{C min}^{-1}$ was most effective for obtaining monodispersed spherical particles during the initial stage of forced hydrolysis in the sulfate system.

Figure 1 shows an example of monodispersed spherical particles having an average size of $0.48 \mu\text{m}$ with a relative standard deviation of 0.09. These particles indicated somewhat broad X-ray powder diffraction peaks attributable to indium(III) hydroxide,¹⁶ being partially comprised of amorphous hydroxide.

Effect of Sulfate Ions on Formation of Monodispersed Indium(III) Hydroxide Particles. The role of the sulfate ions on the precipitation of indium(III) hydroxide was examined by changing the concentration ratio, $[\text{SO}_4^{2-}]_i / [\text{In}^{3+}]_i$, from 0.1 to 3.0 under a fixed nitric acid concentration of $1.0 \times 10^{-3} \text{ mol dm}^{-3}$ at $100 \pm 0.5^\circ \text{C}$ for 120 min. Monodispersed particles were generated at concentration ratios between 1.0 to 1.5 under the given indium(III) concentrations, except for $1.2 \times 10^{-3} \text{ mol dm}^{-3}$, as shown in Fig. 2. Irregularly shaped and/or ellipsoidal particles appeared at concentration ratios less than 1.0, whereas only polydispersed particles formed above 1.5.

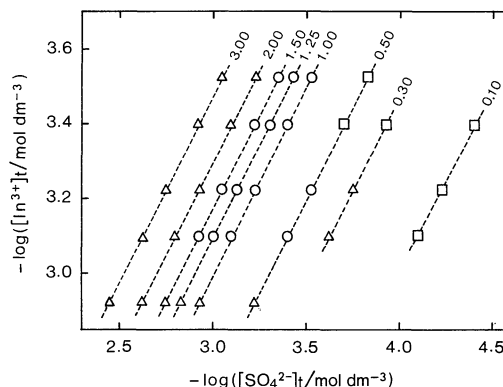


Fig. 2. Effect of concentration ratio, $[\text{SO}_4^{2-}]_i / [\text{In}^{3+}]_i$, on morphology of indium(III) hydroxide particles. Symbols: O; sphere, □; ellipsoidal, and Δ; irregular. Aging conditions: $[\text{In}^{3+}]_i = 6.0 \times 10^{-4} \text{ mol dm}^{-3}$ and $[\text{HNO}_3] = 1.0 \times 10^{-3} \text{ mol dm}^{-3}$ at 100°C for 120 min.

In contrast, the indium(III) nitrate solution, free from sulfate ions, generated cubic particles of well-crystallized indium(III) hydroxide¹⁶ under the conditions shown in Fig. 3a. Octahedral and hexagonal plate particles were also produced, depending on the composition of the starting solution (Figs. 3b and 3c), the latter two kinds of particles being identified as indium(III) sulfate hydroxide hydrate ($\text{InOH}\cdot\text{SO}_4 \cdot 2\text{H}_2\text{O}$)¹⁷ by X-ray powder diffractometry.

In order to gain an overview of the precipitation process, $9.4 \times 10^{-3} \text{ mol dm}^{-3}$ indium(III) nitrate and

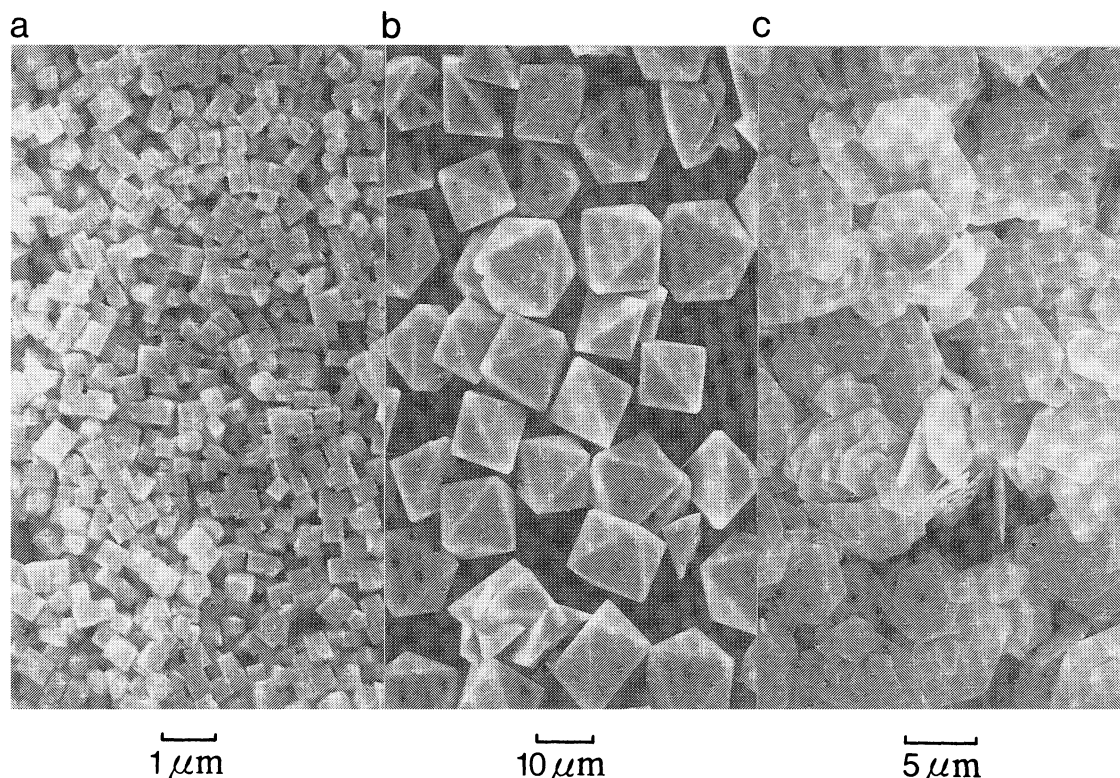


Fig. 3. Scanning electron micrographs of indium(III) hydroxide (a) and sulfate hydroxide hydrate (b and c) particles. Aging conditions: (a) $[\text{In}^{3+}]_i = 6.0 \times 10^{-4} \text{ mol dm}^{-3}$ and $[\text{HNO}_3]_i = 1.0 \times 10^{-3} \text{ mol dm}^{-3}$, (b) $[\text{In}^{3+}]_i = 2.0 \times 10^{-2} \text{ mol dm}^{-3}$, $[\text{HNO}_3]_i = 4.1 \times 10^{-2} \text{ mol dm}^{-3}$, and $[\text{SO}_4^{2-}]_i / [\text{In}^{3+}]_i = 1.9$, and (c) $[\text{In}^{3+}]_i = 2.0 \times 10^{-3} \text{ mol dm}^{-3}$, $[\text{HNO}_3]_i = 2.7 \times 10^{-3} \text{ mol dm}^{-3}$, and $[\text{SO}_4^{2-}]_i / [\text{In}^{3+}]_i = 20$, respectively.

sulfate solutions, containing $2.1 \times 10^{-2} \text{ mol dm}^{-3}$ nitric acid, were titrated very slowly with a $9.5 \times 10^{-3} \text{ mol dm}^{-3}$ potassium hydroxide solution at room temperature. The precipitates appeared during an early stage of titration (pH 3.6, $[\text{OH}^-]_{\text{add}} / [\text{In}^{3+}]_i = 0.33$) in the sulfate solution, in contrast to the case of nitrate solution (pH 4.4, $[\text{OH}^-]_{\text{add}} / [\text{In}^{3+}]_i = 2.5$). A clear difference in the precipitation process indicated that sulfate ions markedly affected the formation of indium(III) hydroxide.

Fractional Changes of Monomeric and Polymeric Indium(III) Species during Forced Hydrolysis. Figure 4 shows the fractional changes of soluble indium(III) species and precipitates during forced hydrolysis of the sulfate solution at $100 \pm 0.5^\circ\text{C}$. The fraction of monomeric species rapidly decreased following deposition of the solids. It was noteworthy that the $[\text{monomer}] / [\text{polymer}]$ ratio, as an indium(III) unit, drastically decreased concomitantly by a sharp fractional maximum of polymeric species during the stage of nucleation of the particles. In addition, a secondary maximum of the fractional change in the polymeric species was also observed at around 110 min, which would arise from a partial dissolution of the particles.

On the other hand, the fraction of polymeric species was quite small during hydrolysis in the nitrate

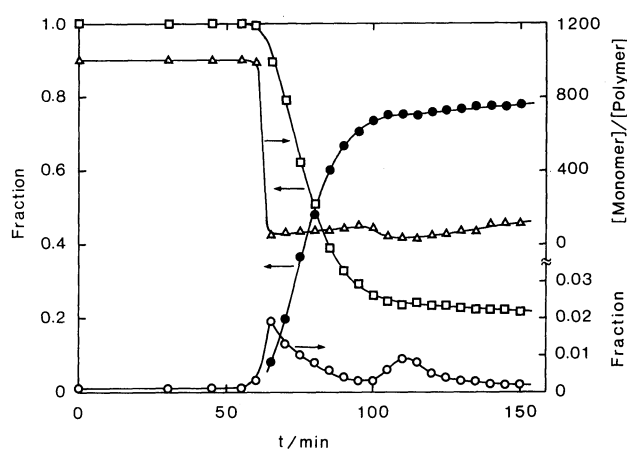


Fig. 4. Fractions of mono- and polynuclear indium(III) species, and precipitates during hydrolysis at 100°C in sulfate system. Symbols: \square ; monomer, \circ ; polymer, \bullet ; precipitate, and Δ ; $[\text{monomer}] / [\text{polymer}]$ ratio. Aging conditions: $[\text{In}^{3+}]_i = 6.0 \times 10^{-4} \text{ mol dm}^{-3}$, $[\text{HNO}_3]_i = 1.0 \times 10^{-3} \text{ mol dm}^{-3}$, and $[\text{SO}_4^{2-}]_i / [\text{In}^{3+}]_i = 1.25$.

solution, though the fraction of monomeric species changed similarly to that in the former system.

Figure 5 shows changes in the size of spherical and cubic particles as a function of the aging time under the same conditions specified in Figs. 1 and 3a,

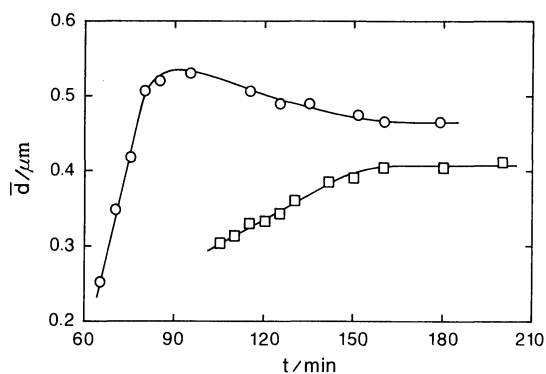


Fig. 5. Changes in size of spherical (O) and cubic (□) particles as a function of aging time at 100°C. Aging conditions: (O) $[\text{In}^{3+}]_i = 6.0 \times 10^{-4} \text{ mol dm}^{-3}$, $[\text{HNO}_3] = 1.0 \times 10^{-3} \text{ mol dm}^{-3}$, and $[\text{SO}_4^{2-}]_i / [\text{In}^{3+}]_i = 1.25$, and (□) $[\text{In}^{3+}]_i = 6.0 \times 10^{-4} \text{ mol dm}^{-3}$ and $[\text{HNO}_3] = 1.0 \times 10^{-3} \text{ mol dm}^{-3}$, respectively.

respectively. The spherical particles grew linearly and then reached a maximum at around 95 min. According to an electron microscopic observation, new crystalline particles originated after this time, implying that the fractional maximum of polymeric species around 110 min (Fig. 4.) arose from a partial dissolution of the particles, leading to secondary nucleation for the new crystalline phase. Similar behavior has been observed in a gallium(III) hydrous oxide system.¹⁰ In contrast, the cubic particles grew normally, as indicated in Fig. 5.

Growth Process of Monodispersed Cubic Indium (III) Hydroxide Particles. The reaction degree, α , is defined as

$$\alpha = (C_0 - C) / (C_0 - C_s), \quad (1)$$

where C_0 , C , and C_s are the initial concentration, the concentration at reaction time t , and the apparent solubility, respectively. If the particles grow through a polynuclear layers process, the following relationship can be obtained as¹⁸⁾

$$t = K_p I_p, \quad (2)$$

where

$$K_p = 0.55 r_f / C_0^p k_m^{1/3} d^{7/3} D^{2/3}, \quad (3)$$

and

$$I_p = \int_0^\alpha x^{-2/3} (1-x)^{-p} dx, \quad p = (m+2)/3. \quad (4)$$

The parameters r_f , m , k_m , d , and D stand for the final size of the particles, the exponent of the concentration dependence for two-dimensional surface nucleation, its apparent rate constant under the given conditions, the height of the surface nuclei, and the diffusion coefficient, respectively.

Figure 6 shows a linear relationship between the reaction time and I_p (taking p as 2, obtained from data

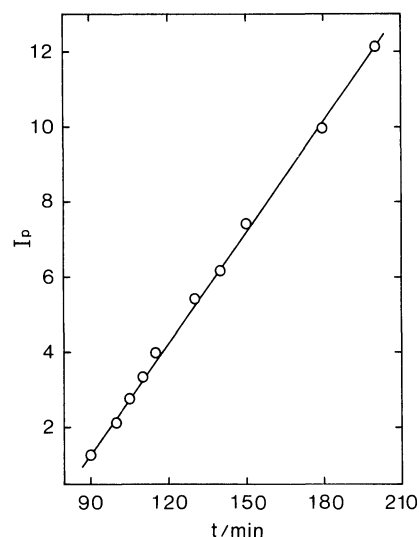


Fig. 6. Plots of integral term, I_p , in Eq. 4 as a function of aging time on cubic particles. Aging conditions: $[\text{In}^{3+}]_i = 6.0 \times 10^{-4} \text{ mol dm}^{-3}$ and $[\text{HNO}_3] = 1.0 \times 10^{-3} \text{ mol dm}^{-3}$.

Table 1. Properties of Indium(III) Hydroxide and Oxide Particles Used for Measurements

Sample	Size	Specific surface area
	μm	$\text{m}^2 \text{g}^{-1}$
Hydroxide (NO_3^-) ^{a)}	0.65	2.3
Oxide (NO_3^-) ^{b)}	0.64	37.2
Hydroxide (SO_4^{2-}) ^{a)}	1.70	23.2
Oxide (SO_4^{2-}) ^{b)}	1.60	100

a) Obtained from indium(III) nitrate and sulfate solutions, respectively. b) Prepared from indium(III) hydroxide by thermal decomposition at 320°C for 3 h.

under the same conditions given in Fig. 3a). The deviation of the intercept from the reaction-time zero would arise from a time lag in the heating and/or the induction period of nucleation. Thus, the indium(III) hydroxide particles grow through polynuclear layers process. The linear growth of cubic particles (Fig. 5) also supported this conclusion. Similar results were obtained for monodispersed spherical particles in a sulfate system.

Points of Zero Charge of Indium(III) Hydroxide and Oxide Particles. The surface properties of the particles were measured by ordinary titration on indium (III) hydroxide and oxide particles made from the nitrate and sulfate systems. The hydroxide particles were repeatedly washed with $2.0 \times 10^{-3} \text{ mol dm}^{-3}$ sodium hydroxide and doubly distilled water in order to remove any species adsorbed on the surfaces of the particles. The oxide particles were then prepared by dehydration at 320°C for 3 h. Table 1 shows the properties of four kinds of the particles thus obtained. The specific surface areas of the oxide particles markedly increased compared with those of the corre-

sponding hydroxide particles, though the oxide particles apparently retained the morphologies of their mother crystals.

The solubilities of the indium(III) hydroxide and oxide particles were estimated to be a function of the pH at $25 \pm 0.1^\circ\text{C}$ and the ionic strength of 0.10 mol dm^{-3} , as shown in Fig. 7. The solubility product, K_{sp} , of the hydroxide particles (the nitrate and sulfate systems) was calculated as being $7.72 \times 10^{-38}\text{ mol}^4\text{ dm}^{-12}$ under these conditions, taking into account the hydrolysis of indium(III) ions at 25°C and the ionic strength of 0.10 mol dm^{-3} ($\text{In}^{3+} + \text{H}_2\text{O} = [\text{InOH}]^{2+} + \text{H}^+$, $*K_1 = 4.90 \times 10^{-5}\text{ mol dm}^{-3}$, $\text{In}^{3+} + 2\text{H}_2\text{O} = [\text{In}(\text{OH})_2]^+ + 2\text{H}^+$, $*\beta_2 = 4.67 \times 10^{-10}\text{ mol}^2\text{ dm}^{-6}$, and $4\text{In}^{3+} + 4\text{H}_2\text{O} = [\text{In}_4(\text{OH})_4]^{8+} + 4\text{H}^+$, $*\beta_{44} = 4.79 \times 10^{-8}\text{ mol dm}^{-3}$).¹⁹ Also, those of the oxide particles were estimated to be 2.68×10^{-36} and $6.35 \times 10^{-36}\text{ mol}^4\text{ dm}^{-12}$ (the sulfate and nitrate systems, respectively) as $1/2\text{In}_2\text{O}_3 + 3/2\text{H}_2\text{O} = \text{In}^{3+} + 3\text{OH}^-$, under the same conditions. These values agreed reasonably well with those reported (1.3×10^{-37} and $1.3 \times 10^{-36}\text{ mol}^4\text{ dm}^{-12}$ at 25°C and the ionic strength of 0 mol dm^{-3} for hydroxide and oxide, respectively).²⁰

Figure 8 shows the surface-charge densities, σ , of the particles as a function of the pH at $25 \pm 0.1^\circ\text{C}$ and an ionic strength of 0.10 mol dm^{-3} , based on titration curves which were corrected²¹ according to the solubilities and dissolution rates of the particles. The points of zero charge (PZC) of the hydroxide and oxide particles made from the nitrate system were estimated as being at the same pH (7.7).

On the other hand, the PZCs of the hydroxide and oxide particles made from a sulfate system were estimated as having a rather low pH (7.0 and 5.4, respectively). If these particles were not alkali-treated, much lower pH values (3.4 and 3.5) were observed as apparent PZCs for the respective particles (the sulfate system). Such low values for the latter samples would

arise from an adsorption of sulfate ions on the surfaces of the particles.²⁰ In fact, sulfate ions were still detectable not only on the surfaces, but as inner inclusions by XPS, even though the particles had been treated with a sodium hydroxide solution.

Discussion

Monodispersed spherical indium(III) hydrous oxide particles were obtained in a limited initial pH range (between 2.9 and 3.2) under given conditions in the sulfate system. Spherical particles of aluminium(III)⁸ and gallium(III)⁹ hydrous oxides with a reasonably narrow size distribution could also be generated in sulfate solutions at specified pH values (4.1 and 2.8, respectively). These pH values for producing monodispersed particles corresponded to trends in the hydrolysis of metal ions, as indicated by the formation constants of first-stage hydrolysis at 25°C , $*K_1$, $9.55 \times 10^{-6}\text{ mol dm}^{-3}$ at $I=0\text{ mol dm}^{-3}$ for aluminium(III),²² $4.90 \times 10^{-5}\text{ mol dm}^{-3}$ at $I=0.10\text{ mol dm}^{-3}$ for indium(III),¹⁹ and $1.20 \times 10^{-3}\text{ mol dm}^{-3}$ at $I=0.5\text{ mol dm}^{-3}$ for gallium(III),²³ respectively.

According to the drastic change in the [monomer]/[polymer] ratio (Fig. 4), the monomeric hydroxoindium(III) complexes would basically act as precursors for the spherical particles, as compared with the cases in gallium(III) sulfate and nitrate solutions.¹⁰ However, the amorphous indium(III) hydrous oxides, resulting from polynuclear hydroxo complexes, were also one of the components of the particles, as judged from the X-ray powder diffraction patterns and the fractional changes of the polymeric species at around 65 min (Fig. 4). Thus, the coprecipitation process of the amorphous hydrous oxides was important for yielding monodispersed spherical particles, even though the particles partially comprised crystalline indium(III) hydroxide.

Polymerized hydroxoindium(III) complexes can

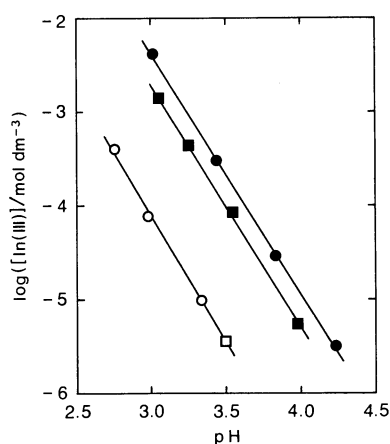


Fig. 7. Solubilities of indium(III) hydroxide and oxide particles at 25°C and $I=0.10\text{ mol dm}^{-3}$. Symbols: O; hydroxide (SO_4^{2-}), \square ; hydroxide (NO_3^-), \bullet ; oxide (SO_4^{2-}), and \blacksquare ; oxide (NO_3^-).

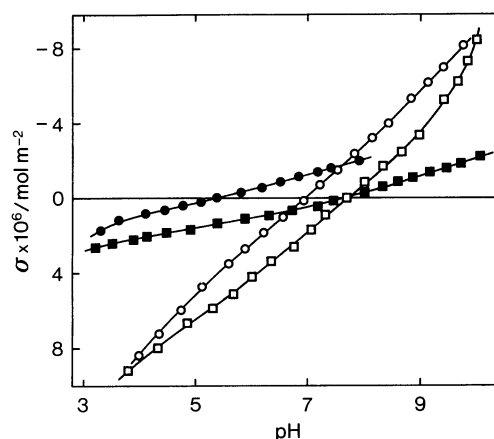


Fig. 8. Surface charge densities of indium(III) hydroxide and oxide particles at 25°C and $I=0.10\text{ mol dm}^{-3}$. Symbols: O; hydroxide (SO_4^{2-}), \square ; hydroxide (NO_3^-), \bullet ; oxide (SO_4^{2-}), and \blacksquare ; oxide (NO_3^-).

easily associate with sulfate ions owing to their large positive charges. The sulfate ions, thus paired, would effectively reduce the positive charge of the polynuclear hydroxo complexes. This, in turn, suggests that the polymers much more easily collide with each other due to less electrostatic repulsion, leading to further polymerization and precipitation. Such a role of the sulfate ions on the precipitation process has been explained in terms of the catalytic action during solid formation.¹¹⁾ The affinity of sulfate ions for metal ions can be compared with the respective formation constants at 25 °C, K_1^{out} , for instance, $19 \text{ mol}^{-1} \text{ dm}^3$ at $I=0.1 \text{ mol dm}^{-3}$ for aluminium(III)²⁴⁾ and $60 \text{ mol}^{-1} \text{ dm}^3$ at $I=2 \text{ mol dm}^{-3}$ for indium(III),²⁵⁾ though they exist as outer-sphere complexes.²⁶⁾

The concentration ratio of the total sulfate to indium(III) ions was indicated as being an important factor, ranging from 1.0 to 1.5 (Fig. 2), to make monodispersed spherical particles. On the other hand, monodispersed spherical particles of aluminium(III) and gallium(III) hydrous oxide have been obtained at rather wide concentration ratios, 1.0–2.0 for aluminium(III) and 0.6–2.0 for gallium(III), respectively,^{8,9)} which would depend on the affinity and concentration of sulfate ions.

In addition, an appropriate formation rate of the polynuclear hydroxo complexes is essential in order to obtain a suitable supersaturation, leading to a proper nucleation rate, whereas hydrolysis generally takes place faster than condensation.²⁷⁾ These conditions have been required as the starting composition of the solution and the heating rate.⁹⁾

References

- 1) J. H. L. Watson, R. R. Cardell, Jr., and W. Heller, *J. Phys. Chem.*, **66**, 1757 (1962).
- 2) E. Matijević and P. Scheiner, *J. Colloid Interface Sci.*, **63**, 509 (1978).
- 3) E. Matijević, *Acc. Chem. Res.*, **14**, 22 (1981).
- 4) E. Matijević, *Ann. Rev. Mater. Sci.*, **15**, 483 (1985).
- 5) S. Hamada and E. Matijević, *J. Colloid Interface Sci.*, **84**, 274 (1981).
- 6) S. Hamada and E. Matijević, *J. Chem. Soc., Faraday Trans. I*, **78**, 2147 (1982).
- 7) E. Matijević, A. D. Lindsay, S. Kratochvil, M. E. Jones, R. I. Larson, and N. W. Cayey, *J. Colloid Interface Sci.*, **36**, 273 (1971).
- 8) R. Brace and E. Matijević, *J. Inorg. Nucl. Chem.*, **35**, 3691 (1973).
- 9) S. Hamada, K. Bando, and Y. Kudo, *Nippon Kagaku Kaishi*, **1984**, 1068.
- 10) S. Hamada, K. Bando, and Y. Kudo, *Bull. Chem. Soc. Jpn.*, **59**, 2063 (1986).
- 11) H. de Hek, R. J. Stol, and P. L. de Bruyn, *J. Colloid Interface Sci.*, **64**, 72 (1978).
- 12) A. Bell and E. Matijević, *J. Inorg. Nucl. Chem.*, **37**, 907 (1975).
- 13) M. Iwase, T. Yotsuyanagi, and M. Nagayama, *Nippon Kagaku Kaishi*, **1968**, 49.
- 14) Y. Nishikawa, K. Hiraki, S. Gohda, K. Nakagawa, and M. Tamura, *Nippon Kagaku Kaishi*, **1975**, 1479.
- 15) M. Iwase, T. Yotsuyanagi, and M. Nagayama, *Nippon Kagaku Kaishi*, **1985**, 2271.
- 16) R. Roy and M. W. Shafer, *J. Phys. Chem.*, **58**, 372 (1954).
- 17) G. Johansson, *Acta Chem. Scand.*, **15**, 1437 (1961).
- 18) A. E. Nielsen, "Kinetics of Precipitation," Pergamon Press, Oxford (1964), Chaps. 3 and 4.
- 19) P. L. Brown, J. Ellis, and R. N. Sylva, *J. Chem. Soc., Dalton Trans.*, **1982**, 1911.
- 20) W. Feitknecht and P. Schindler, *Pure Appl. Chem.*, **6**, 130 (1963).
- 21) C. P. Huang, "Adsorption of Inorganics at Solid-Liquid Interface," ed by M. A. Anderson and A. J. Rubin, Ann Arbor Science Publishers (1981), p. 183.
- 22) C. R. Frink and M. Peech, *Inorg. Chem.*, **2**, 473 (1963).
- 23) A. S. Wilson and H. Taube, *J. Am. Chem. Soc.*, **74**, 3509 (1952).
- 24) M. Eigen and K. Tamm, *Z. Elektrochem.*, **66**, 107 (1962).
- 25) E. N. Deichman, G. V. Rodicheva, and L. S. Kryina, *Zh. Neorg. Khim.*, **11**, 2237 (1966).
- 26) R. E. Hester and R. A. Plane, *Inorg. Chem.*, **3**, 769 (1964).
- 27) K. H. Lieser, *Angew. Chem., Int. Ed. Engl.*, **8**, 188 (1969).